MOLECULAR AND CELLULAR BIOLOGY, Dec. 1992, p. 5311–5318
0270-7306/92/125311-08$02.00/0

Vol. 12, No. 12

Transcription Enhances Intrachromosomal Homologous Recombination in Mammalian Cells

JAC A. NICKOLOFF

Department of Cancer Biology, Harvard University School of Public Health, Boston, Massachusetts 02115

Received 4 May 1992/Returned for modification 24 June 1992/Accepted 31 August 1992

The influence of transcription on homologous intrachromosomal recombination between direct and inverted repeats has been examined by using Chinese hamster ovary cells. Recombination was monitored between two integrated neomycin (*neo*) genes, including one silent allele and a second allele regulated by the inducible mouse mammary tumor virus promoter. Transcription of mouse mammary tumor virus *neo* alleles was regulated with the glucocorticoid hormone dexamethasone. Alleles transcribed at high levels recombined about two- to sevenfold more frequently than identical alleles transcribed at low levels. Direct repeats recombined primarily by a gene conversion mechanism; inverted repeats produced a variety of rearranged products. These results are discussed in relation to recombinational processes that regulate gene expression, influence gene family structures, and mediate genomic instability associated with cellular transformation and tumorigenesis.

Homologous recombination levels have been correlated with transcription levels in both yeast and mammalian cells. Evidence for enhanced recombination in transcriptionally active DNA in the yeast *Saccharomyces cerevisiae* was first obtained by Keil and Roeder (13) during a search for recombination hot spots. This search led to the isolation of *HOT1*, which mapped to the rRNA gene cluster. *HOT1* enhanced homologous recombination between nearby duplicated genes by 5- to 10-fold. Linker insertion mutagenesis of *HOT1* demonstrated that the recombination-stimulating activity correlated with its capacity to promote transcription by RNA polymerase I (25). In diploids, *HOT1* stimulates interchromosomal gene conversion (29, 30). RNA polymerase II-mediated transcription driven from the *GAL1-10* promoter was also shown to enhance mitotic intrachromosomal recombination between nontandem duplications. These studies showed that transcription of only one duplicated element was required to stimulate recombination by a crossover mechanism (26). In the fission yeast *Schizosaccharomyces pombe*, meiotic and mitotic interchromosomal recombinations are enhanced by the highly active *ADH1* promoter (9).

Although there is direct evidence that transcription enhances extrachromosomal recombination in mammalian cells (19), only indirect evidence has been reported for mammalian chromosomal loci. Alt and coworkers found that immunoglobulin gene rearrangements were immediately preceded by increased transcriptional activity (1, 2). These results were explained by a model suggesting that transcriptionally active (open) DNA conformations are more accessible to nuclease attack. Further indirect evidence that transcription enhances homologous recombination in mammalian cells has come from gene targeting studies (11, 18) and from studies of the meiotic recombination hot spot in the mouse Eβ gene (23).

The mechanism of transcription-enhanced recombination is not understood. However, in yeasts it is dependent on the *RAD52* gene product, which is involved in double-strand break repair, suggesting a role for double-strand breaks (17, 27). Studies of yeast mating type interconversion support this notion. Recombination at mating type loci is initiated by HO nuclease-mediated double-strand cleavage of the transcriptionally active *MAT* locus; the homologous, but transcriptionally silent, *HML* and *HMR* loci are not cleaved by HO nuclease. As suggested for immunoglobulin rearrangements, transcriptionally active *MAT* DNA was hypothesized to be more accessible to enzymatic cleavage than silent DNA (15).

This report describes studies of transcriptional effects on intrachromosomal recombination between duplicated neomycin (*neo*) genes stably integrated into CHO chromosomes. Transcription of one *neo* gene was controlled by the dexamethasone (DEX)-responsive mouse mammary tumor virus (MMTV) promoter (21). Recombination levels were enhanced two- to sevenfold when transcription was induced with DEX relative to levels with identical, less active alleles, providing direct evidence that transcription enhances intrachromosomal recombination in mammalian cells. Recombination between direct repeats was mediated primarily by a gene conversion mechanism. In contrast, recombination between inverted repeats produced a variety of rearranged products.

MATERIALS AND METHODS

Plasmids. Standard procedures were used for molecular cloning (22). Plasmid DNAs were prepared as described previously (5). Derivatives of plasmid pMSGneo (19) were produced in several steps. Both *Hin*dIII sites were destroyed by cleaving pMSGneo with *Hin*dIII, filling in the 4-bp extension with T4 DNA polymerase, and ligating with T4 DNA ligase. Frameshift mutations were introduced into *neo* in the resulting plasmid (pMSGneoΔH3) by inserting 10-bp *Hin*dIII linkers (New England Biolabs) into either the *Msc*I site or a filled-in *Bss*HII site, producing pMSGneoH(Msc) and pMSGneoH(Bss), respectively. An *Eco*RI-linked *Hin*dIII-*Sma*I fragment of pSV2neo (24) carrying *neo* coding sequences, but lacking mammalian promoter and transcription termination signals, was produced by replacing the *Hin*dIII site in plasmid pneo (19) with *Eco*RI linkers. This 1,200-bp *neo* fragment was inserted into the *Eco*RI site in pMSGneoH(Bss) and pMSGneoH(Msc), and four derivatives (called pMSGneo^2) were isolated with direct or inverted *neo* duplications.

Construction and characterization of CHO cell lines with heteroallelic *neo* genes. Cell culture and electroporation con-

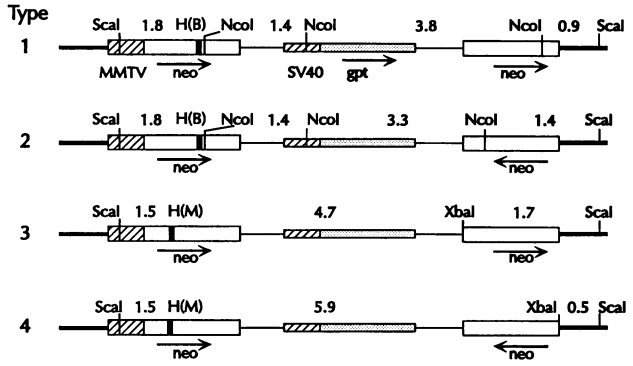

FIG. 1. Structures of integrated recombination substrates. Two copies of the 1,200-bp *neo* coding fragment were present either as direct or inverted repeats (open boxes). *Hin*dIII linker insertion mutations in either *Msc*I sites [H(M)] or *Bss*HII sites [H(B)] are shown by dark bars. pBR322 DNA is shown by thick lines. Strains carry either direct repeats (types 1 and 3) or inverted repeats (types 2 and 4). MMTV *neo* genes have either 3′ mutations (types 1 and 2) or 5′ mutations (types 3 and 4). Distances between sites are shown in kilobase pairs; the *Nco*I site in *neo* is 36 bp from the *Bss*HII site. *Sca*I-*Nco*I fragments shown for strain types 1 and 2 are identical in types 3 and 4, respectively. *Xba*I sites shown for strain types 3 and 4 are identical in types 1 and 2, respectively.

ditions were described previously (19). From 0.1 to 1 μg of the four pMSGneo[2] derivatives were linearized with *Nde*I and electroporated into CHO strain K1c, producing MAX-resistant (MAX^r) transfectants that were characterized by Southern hybridization analysis as previously described (19). Total RNA was prepared from cultures inoculated with 1×10^6 to 1.5×10^6 cells in 100-mm (diameter) dishes incubated for at least 2 days. RNA preparations and Northern (RNA) hybridization analyses were performed as previously described (19).

Recombination assays. Recombination frequencies were determined with independently derived populations of parent cell lines. Independent populations were produced by seeding parent cells at low densities in 6-well dishes, incubating for 7 days, transferring single colonies from each well to 100-mm dishes, and expanding until confluent. Cells were harvested and quantified with a Coulter counter, and 6×10^6 cells were plated in six 100-mm dishes in medium containing G418 (500 μg/ml; active concentration, 520 μg/mg). DEX (1 μM, unless otherwise noted) was added to half of the dishes immediately after inoculations, and dishes were not disturbed during an 11-day incubation to avoid dislodging cells. G418-resistant (G418^r) colonies were stained with 1% crystal violet in 70% ethanol and counted. Recombinant colonies were counted only when greater than 50 cells; smaller colonies were not counted, as these may have arisen from cells detaching from the plate and reattaching at a different position. Plating efficiencies were similar in the presence and absence of DEX. Recombination frequencies were calculated as the number of G418^r colonies formed per cell plated.

RESULTS

Cell lines with inducible heteroallelic *neo* genes. The effects of transcription on recombination were investigated with four types of strains carrying integrated *neo* heteroallele duplications flanking a selectable *Escherichia coli gpt* gene driven by the simian virus 40 (SV40) early promoter (SV*gpt*) (Fig. 1). One *neo* allele, regulated by the inducible MMTV promoter, was inactivated by linker frameshift mutations in either 5′ or 3′ positions (*Msc*I or *Bss*HII sites, respectively). The second *neo* allele had wild-type coding sequences but was nonfunctional because it lacked a promoter. Integrated recombination substrates were predicted to produce G418^r recombinants by several mechanisms including gene conversions of MMTV *neo*, crossovers between *neo* genes, or unequal sister chromatid exchanges in G2. Gene conversion products of all strain types were expected to retain parental structures, losing only the mutation sites in MMTV *neo* alleles. Crossovers between direct repeats (strain types 1 and 3) were predicted to delete SV*gpt* genes, producing recombinants sensitive to MAX medium (MAX^s); unequal exchanges yield either *neo* triplications with two SV*gpt* genes (MAX^r) or MAX^s products indistinguishable from those formed by crossovers. Crossovers and unequal exchanges between inverted repeats (strain types 2 and 4) were predicted to invert the SV*gpt* gene. Therefore, all G418^r recombinants of inverted-repeat strains were expected to remain MAX^r. Structures of recombinant products could be confirmed by Southern hybridization analysis.

Ten independent MAX^r transfectants of each strain type were screened for resistance to G418 to eliminate those that had undergone a successful recombination event during transfection. Consistent with the results of Lin et al. (16), plasmids with inverted repeats produced more G418^r recombinants during transfection than those with direct repeats (50 versus 15%, respectively). On the basis of Southern hybridization analysis of all MAX^r G418^s transfectants, two isolates of each strain type were selected for further characterization (Fig. 2). Seven strains carried single copies of intact recombination substrates. The remaining strain (designated 2-3) apparently had integrated *neo*-SV*gpt*-*neo* sequences separated from the MMTV promoter. Northern analysis showed that treatment with DEX greatly increased the amount of *neo* mRNA in all strains, except strain 2-3 (representative data are shown in Fig. 3). Although direct measurements of transcription rates were not made, it is well established that increased amounts of mRNA produced from MMTV promoter-driven genes in cells treated with DEX result from increased rates of transcription (21, 34). Therefore, measurements of *neo* mRNA levels by Northern analysis are likely to accurately reflect MMTV *neo* transcription rates.

To measure reversion frequencies of mutant MMTV *neo* alleles, analogous strains that lacked silent copies of *neo* were constructed. The presence of intact, integrated plasmids was confirmed as above for four isolates, including two each with mutations in *Msc*I and *Bss*HII sites (data not shown). Reversion of MMTV *neo* alleles in these control strains was measured by plating 3×10^6 cells in G418 medium with or without DEX in standard assays (Materials and Methods). Reversion frequencies in the presence or absence of DEX were $\leq 0.33 \times 10^{-6}$.

Expression of MMTV *neo*$^+$ alleles in the absence of DEX is sufficient to confer G418 resistance. Since recombination between heteroallelic *neo* genes transcribed at low levels was monitored by selection for G418^r colonies in medium lacking DEX, it was important to demonstrate that single MMTV *neo*$^+$ genes are expressed at sufficient levels in the absence of DEX to confer the G418^r phenotype. This was demonstrated in a transfection-based assay system (19) and is supported by two sets of control experiments with the strains used in this study. First, all eight strains shown in Fig. 2 yielded G418^r colonies in the absence of DEX.

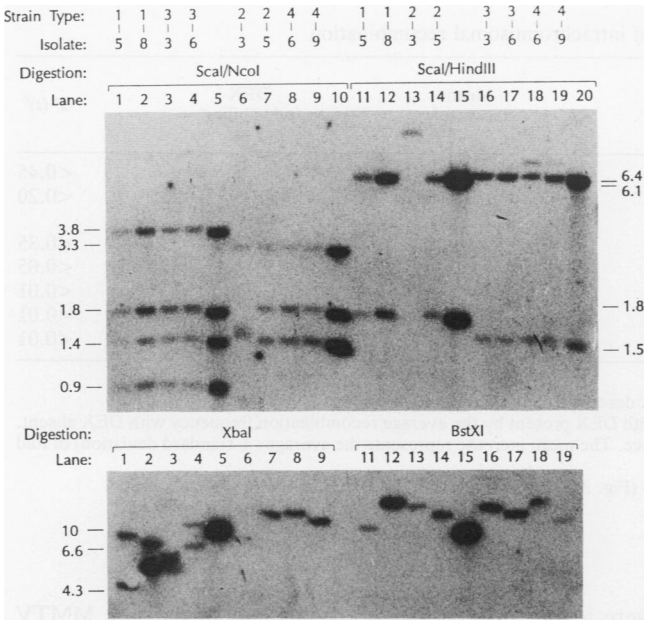

FIG. 2. Southern analysis of integrated *neo* heteroalleles. Approximately 10 μg of genomic DNA from each of eight strains containing integrated derivatives of pMSGneo[2] was digested with the indicated enzymes, separated on a 0.8% agarose gel, transferred to a nylon membrane, and hybridized with a ^{32}P-labeled *neo* probe. Control digests of appropriate pMSGneo[2] derivatives are present in lanes 5, 10, 15, and 20. Control lanes contain 40 pg of plasmid DNA, an amount equivalent to about four integrated copies. Sizes of control DNA fragments are listed in kilobase pairs; fragment identities are shown in Fig. 1. (Top) *Sca*I sites present within MMTV promoter and pBR322 sequences allow excision of integrated plasmids nearly intact. *Nco*I cleaves asymmetrically within *neo* and is therefore diagnostic for direct and inverted repeats. Both yield fragments of 1.8 and 1.4 kbp. Direct repeats also yield 3.8- and 0.9-kbp fragments, and inverted repeats yield a 3.3-kbp fragment and a second 1.4-kbp fragment. *Hin*dIII linker insertions within MMTV *neo* alleles are verified by *Hin*dIII digests. Strain types 1 and 2 yield 6.1- and 1.8-kbp fragments; types 3 and 4 yield 6.4- and 1.5-kbp fragments. (Bottom) Because *Xba*I cleaves recombination substrates once, *Xba*I digests are diagnostic for single-copy integrants. Inverted and direct repeats should produce one or two hybridizing *Xba*I fragments of indeterminant size, respectively (Fig. 1). All strains lack an *Xba*I fragment equal to the 10-kbp linear size of pMSGneo[2] (lane 5, cleaved with *Xba*I) and are therefore single-copy integrants. *Bst*XI does not cleave within the integrated DNA. A single *Bst*XI fragment larger than linearized pMSGneo[2] (lane 15, cleaved with *Xba*I) is diagnostic for plasmids integrated at a single chromosomal locus.

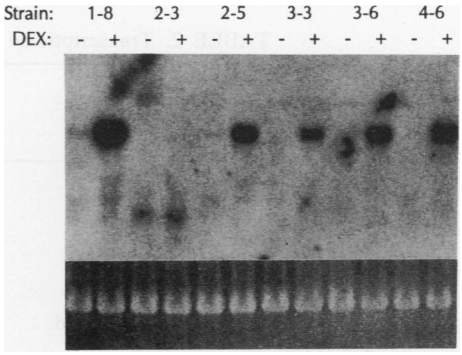

FIG. 3. DEX-induced transcription of MMTV *neo*. For each strain, 10^6 cells were plated on two 100-mm (diameter) dishes and incubated for 24 h. DEX was added to half of the dishes to a final concentration of 1 μM, the cells were incubated for 24 h, and total cellular RNA was prepared. Northern hybridization was performed with a ^{32}P-labeled *neo* probe. Equal loading is shown below in a photograph of ethidium bromide-stained 18S rRNA. Upon longer exposure, faint signals are detectable in the absence of DEX for each strain except 2-3 (data not shown).

Structural analysis of recombinant products (described below) confirmed the presence of single MMTV *neo*$^+$ genes. Second, reconstruction experiments were performed with 10 G418^r (MAX^r or MAX^s) recombinants from strains 3-3, 3-6, 4-6, and 4-9 that had arisen in the presence or absence of DEX. Approximately 200 cells of each recombinant were inoculated into three dishes containing either nonselective medium, G418 medium, or G418 medium with DEX. In each case, similar numbers of colonies arose on selective and nonselective dishes (Table 1). To mimic the experimental conditions used to monitor recombination, reconstruction experiments were repeated with selective medium containing 10^6 cells of the corresponding parental lines (i.e., G418^s MAX^r cells). The number of additional recombinants produced from 10^6 cells of each of the four parent strains was determined independently in parallel dishes lacking G418^r recombinant cells, and these background recombination values were subtracted from experimental values. There were no significant differences between the numbers of colonies formed in the presence and absence of DEX (Table 1). These experiments demonstrate that MMTV *neo*$^+$ alleles are transcribed at sufficient levels to confer G418^r in the absence of DEX.

Intrachromosomal recombination frequencies are proportional to transcription levels. Recombination frequencies were determined in at least four independently derived populations of the eight strains described in Fig. 2 (see

TABLE 1. Plating efficiencies of recombinant products in selective and nonselective media

Parent (*n*)[a]	Plating efficiency				
	Nonselective[b]	G418[b]	G418+DEX[b]	With 10^6 parent cells[c]	
				G418	G418+DEX
3-3 (2)	100 ± 2	101 ± 26	83 ± 13	81 ± 13	91 ± 17
3-6 (3)	100 ± 13	104 ± 21	70 ± 22	53 ± 10	62 ± 15
4-6 (2)	100 ± 13	83 ± 6	75 ± 2	31 ± 22	38 ± 12
4-9 (3)	100 ± 39	77 ± 19	83 ± 12	61 ± 12	85 ± 33

[a] *n*, number of G418^r recombinants tested. Both strain 3-3 recombinants were MAX^r; one arose without DEX, one arose with DEX. Two of three from strain 3-6 were MAX^r; one each arose with and without DEX, and the MAX^s recombinant arose without DEX. One strain 4-6 recombinant was MAX^s and arose without DEX, and one was MAX^r and arose with DEX. Two of three from strain 4-9 were MAX^r; one each arose with and without DEX, and the MAX^s recombinant arose with DEX.

[b] Equal numbers of cells of each recombinant were seeded in the three types of media. For each experiment, the number of colonies formed under selective conditions was normalized to values with nonselective medium, which were assigned a value of 100. Averages (± standard deviations) are given for products of strains 3-6 and 4-9; averages (± ranges) are given for products of strains 3-3 and 4-6.

[c] Results with 10^6 parent cells mixed with recombinant cells prior to plating; recombination levels for each parent strain were independently determined and subtracted from observed values. These corrected values were then normalized to values with nonselective medium; averages and variations are presented for products of each strain as described above.

TABLE 2. Transcriptional enhancement of intrachromosomal recombination

Strain (n^a)	Recombination frequency[b] (10^6)		Fold increase[c]	Mean increase[d]	DEX inducibility[e]	$P(t)^f$
	DEX absent	DEX present				
1-5[g] (5)	0.3 ± 0.1	1.0 ± 1.0	3.0	3.0 ± 3.5	+	<0.45
1-8 (4)	2.8 ± 3.1	8.8 ± 7.3	3.1	6.6 ± 4.6	+	<0.20
2-3 (5)	5.5 ± 4.4	0.2 ± 0.3			−	
2-5 (4)	5.9 ± 1.5	8.1 ± 4.2	1.4	1.5 ± 0.7	+	<0.35
3-3 (5)	3.1 ± 1.4	6.1 ± 2.3	2.0	2.4 ± 1.4	+	<0.05
3-6 (5)	4.4 ± 2.0	13.8 ± 5.4	3.1	3.7 ± 2.3	+	<0.01
4-6 (5)	2.8 ± 1.3	19.3 ± 10.6	6.9	7.5 ± 4.8	+	<0.01
4-9 (4)	4.5 ± 1.3	12.5 ± 4.1	2.8	3.0 ± 1.2	+	<0.01

[a] *n*, number of independent determinations.
[b] Average recombination frequencies (± standard deviations) were determined as described in Materials and Methods.
[c] Fold increase was calculated by dividing the average recombination frequency with DEX present by the average recombination frequency with DEX absent.
[d] Fold increases for each independent population were calculated as described above. The mean increase represents the average (± standard deviation) of fold increase values independently determined for each population of each strain type.
[e] DEX inducibility of *neo* transcription was monitored by Northern hybridization (Fig. 3).
[f] Probability values from *t* test.
[g] Strain 1-5 grows slowly and is tetraploid.

Materials and Methods). Because cultures were split into separate dishes immediately before DEX was added to half of the dishes, the number of preexisting recombinants was internally controlled for each independent population of each strain tested. Background recombination frequencies are expected to vary among independent populations of each strain because of variations in the rate of recombination and in the timing of events during culture expansion, with very early events producing "jackpots." These variations are exhibited as large standard deviations. Therefore, recombinants existing within any single population of cells at the time of plating may or may not have resulted from independent recombination events. In analyses of recombinant products (see below), recombinants were considered to have arisen independently when derived from independent populations of parent strains. Alternatively, independence can be established for products with different phenotypes (i.e., MAX^r or MAX^s) or different genotypes (e.g., crossovers and gene conversions).

All strains, except 2-3, exhibited enhanced recombination when transcription was stimulated with DEX (Table 2). Thus, transcription stimulated recombination between both direct and inverted repeats. The increased recovery of $G418^r$ recombinants in DEX-treated cultures is due to increased numbers of independent events, since cultures were not disturbed following the application of G418-selective pressure (the observed DEX-dependent increase in recombinants does not depend on the independence of background recombinants). Increases are quantitated in Table 2 as the ratio of the average recombination frequencies for DEX-treated and untreated cultures (fold increase). Increases in recombination frequencies are significant with strain types 3 and 4 [$P(t) < 0.05$], but significance cannot be established for the three remaining strains with intact recombination substrates because of low levels of enhancement and large standard deviations. However, consistent increases in recombination were observed in these three strains, shown by averages of independently determined increases of all populations tested for individual strains (Table 2, mean increase). These latter values provide a measure of the variability of DEX-dependent increases among independent populations.

To rule out the possibility that DEX stimulates recombination nonspecifically, control strains (called $SVneo^2$) which were identical to $MSGneo^2$ strains except that the MMTV promoter was replaced with an SV40 promoter were constructed. As above, *neo* alleles flank SV*gpt*. The structures of integrated $SVneo^2$ recombination substrates were characterized, and recombination assays were performed as described above. As found with analogous control experiments involving extrachromosomal recombination substrates (19), DEX reduced recombination frequencies in $SVneo^2$ strains (data not shown). It was shown by Northern analysis that DEX reduced transcript levels of SV40 promoter-driven genes (19). If these reduced transcript levels reflect reduced transcription rates, such reductions can explain the observed DEX-dependent reductions in extra- and intrachromosomal recombination between SV40 promoter-driven genes. These control experiments demonstrate that DEX-enhanced recombination between *neo* alleles in $MSGneo^2$ strains depends on the presence of the MMTV promoter.

To characterize the kinetics of DEX-induced transcription, two analyses were performed. First, *neo* transcript levels were monitored in cells exposed to DEX for increasing times. DEX increased *neo* mRNA levels within 30 min, with maximum levels reached in about 4 h. Within 24 h, *neo* mRNA levels decreased about fivefold below maximum levels (Fig. 4) and continued to decrease between 24 and 48 h (5a). A pulse-chase experiment indicated that treatment with DEX increases *neo* transcript levels for several hours after DEX is removed from culture media (Fig. 4). These results suggest that recombination is stimulated within 24 h after DEX addition.

The mechanism of transcription-enhanced recombination was explored by characterizing independent recombinant products of direct and inverted repeat strains by using genetic and physical assays. $G418^r$ recombinants were first tested for resistance to MAX medium. With direct repeat strains, about 90% of $G418^r$ recombinants remained MAX^r (Table 3). Southern analyses confirmed that MAX^r recombinants lost the *Hin*dIII linker mutation, consistent with a gene conversion mechanism; MAX^s recombinants had deleted SV*gpt*, as expected for crossover or unequal exchange events (Fig. 5). Inverted-repeat strains yielded several unexpected results. As shown in Fig. 6, products of gene conversions, crossovers, and unequal sister chromatid exchanges with inverted repeats were predicted to retain SV*gpt* and remain MAX^r. Surprisingly, about 15% of invert-

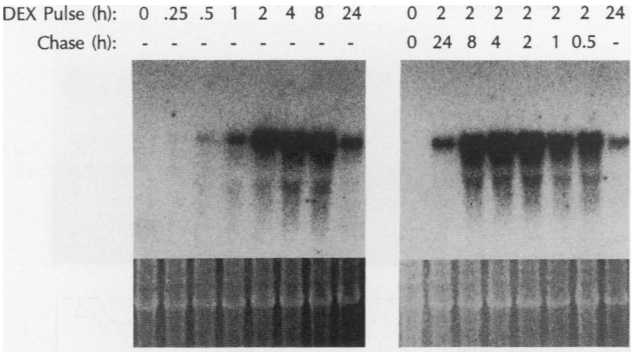

FIG. 4. Kinetics of DEX-induced transcription. Total cellular RNA prepared from strain 4-6 cells was blotted and hybridized as described in Fig. 3. DEX was added for the indicated pulse times. Medium with DEX was either removed and replaced with normal medium for the indicated chase times (right panel) or was not removed (left panel). Similar patterns were obtained when G418 was added simultaneously with DEX (data not shown).

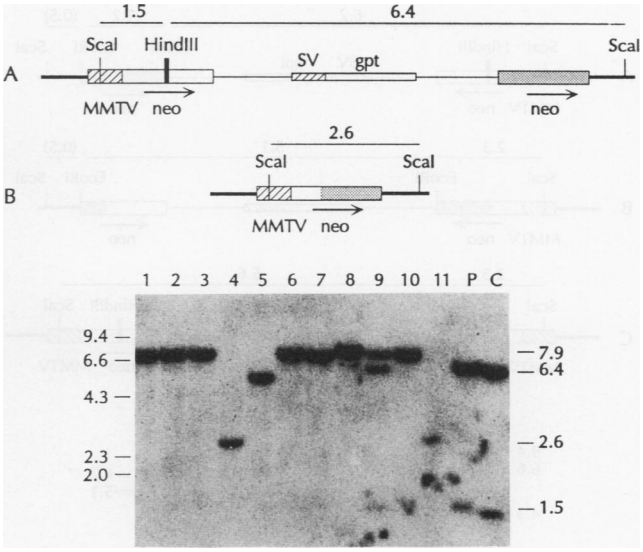

FIG. 5. Direct-repeat recombination products. (Top) Restriction maps of the parent recombination substrate (A) and the predicted structure of a crossover product (B) for strain 3-6. *neo* alleles are shaded differently so that their positions in the crossover product are apparent. Fragment sizes are given in kilobase pairs. (Bottom) Genomic DNAs from eleven G418^r recombinants of strain 3-6 were digested with *Sca*I and *Hin*dIII and analyzed as described in the legend to Fig. 2 (lanes 1 to 11). Lanes P and C, genomic parental DNA and control plasmid DNA, respectively, digested with *Sca*I and *Hin*dIII. MAX^r products lose the *Hin*dIII linker mutation and yield a single 7.9-kbp fragment (lanes 1 to 3 and 6 to 10). MAX^s crossover products lose the SV*gpt* gene yielding a single 2.6-kbp fragment (lanes 4 and 11). An unusual rearrangement is present in lane 5; both parental and gene conversion patterns are found in lane 9, consistent with a nondisjunction event and subsequent gene conversion. Recombinants in lanes 1, 3, 5, 7, and 10 arose without DEX; the remainder arose with DEX.

ed-repeat recombinants were MAX^s (Table 3). Southern patterns of 11 inverted-repeat recombinants did not match predicted restriction patterns (Fig. 6). Additional mapping indicated that these 11 products had at least eight different structures (data not shown). Most MAX^s products carried a 5.1-kbp *Eco*RI-*Sca*I fragment diagnostic for crossovers, suggesting that SV*gpt* genes may be inverted in these products. It is possible that inversions of SV*gpt* influence SV*gpt* expression (see Discussion).

Comparisons of DEX-induced recombination frequencies and DEX-induced transcript levels for strains carrying identical recombination substrates, such as strains 3-3 and 3-6 (Fig. 3 and Table 2) and strains 4-6 and 4-9 (data not shown), suggested that recombination levels might vary continuously with transcription levels. This possibility was investigated by monitoring transcript and recombination levels in strain 4-6 cells exposed to various concentrations of DEX. Strain 4-6 was chosen for this analysis because it gave the highest enhancement of recombination with DEX (Table 2) and would therefore provide the greatest sensitivity. The results of this experiment, shown in Fig. 7, indicate that intrachromosomal recombination frequencies are proportional to transcription levels in this strain. Although full dose-response curves were not obtained with other strains, the data shown in Table 2 and Fig. 3 represent two-point dose-response curves. In light of these results, it is likely that these strains would exhibit similar dose-response curves since various concentrations of DEX would be expected to elicit similar responses in MMTV promoter-driven genes in clonal derivatives of CHO K1c cells.

TABLE 3. Genetic analysis of G418^r recombinant products

Strain	*neo* orientation	No. of recombinant products			
		DEX absent		DEX present	
		MAX^s	MAX^r	MAX^s	MAX^r
3-3	Direct	0	11	0	12
3-6	Direct	1	10	2	10
4-6	Inverted	3	9	3	9
4-9	Inverted	0	8	1	11

DISCUSSION

Transcriptional enhancement of recombination. There is substantial evidence indicating that transcription enhances recombination in yeasts. Only indirect evidence for such an effect at mammalian chromosomal loci has been reported previously (1, 2, 11, 18, 23). The present study provides direct evidence for a correlation between intrachromosomal recombination levels and transcription levels in mammalian cells. Transcription enhances recombination between direct and inverted repeats and requires transcriptional activity in only one repeat. Preliminary data indicate that similar effects are found when both repeats are transcriptionally active (5a). Recombination levels varied between alleles transcribed at both high and low levels among strains used in this study, even among strains harboring identical recombination substrates. Such differences might reflect variations in basal or induced transcription levels in different chromosomal environments. Alternatively, chromosomal environments might influence recombination independently of transcription.

Similar recombinant product spectra were found with alleles transcribed at high and low levels. This suggests that transcription influences recombination frequencies but not recombination mechanisms. Recombinant products of direct repeats arose primarily by a gene conversion mechanism, as found in several studies with yeasts (9, 28–30). However, two studies with yeasts involving a single-promoter system

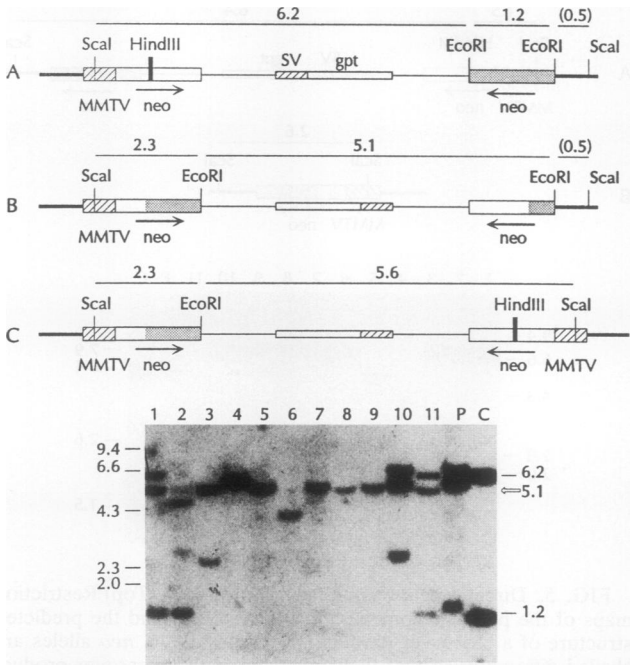

FIG. 6. Inverted-repeat recombination products. Symbols are as described in the legend to Fig. 5. (Top) Restriction maps of the parent recombination substrate (A), crossover (B), and unequal sister chromatid exchange products (C). The 0.5-kbp *Eco*RI-*Sca*I fragment does not hybridize with the *neo* probe. Gene conversions yield parent structures lacking the *Hin*dIII site. As diagrammed in panel B, crossovers may have associated gene conversions. (Bottom) Genomic DNAs from 11 G418^r recombinants of strain 4-6 were digested with *Sca*I and *Eco*RI (lanes 1 to 11). Parent (lane P) and plasmid control (lane C) DNAs differ by the presence of a 5.1-kbp fragment (arrow), possibly because of an early rearrangement during culture expansion in the particular population used to prepare the parent DNA sample. Genomic DNA originally isolated from strain 4-6 (shown in Fig. 2) exhibited normal patterns. Several other digestion patterns (*Eco*RI, *Hin*dIII, *Sca*I, *Hin*dIII-*Sca*I, and *Eco*RV) indicated that the 5.1-kbp fragment is not a partial digestion fragment (5a). Isolates in lanes 1 to 3, 10, and 11 were MAX^r; the remainder were MAX^s. Recombinants in lanes 1, 2, 4, 6, 9, and 10 arose without DEX; the remainder arose with DEX. DNA in lanes containing greater amounts of genomic DNA migrates slightly more slowly than plasmid DNA or smaller amounts of genomic DNA; this is a "salt effect" artifact of loading large amounts of DNA.

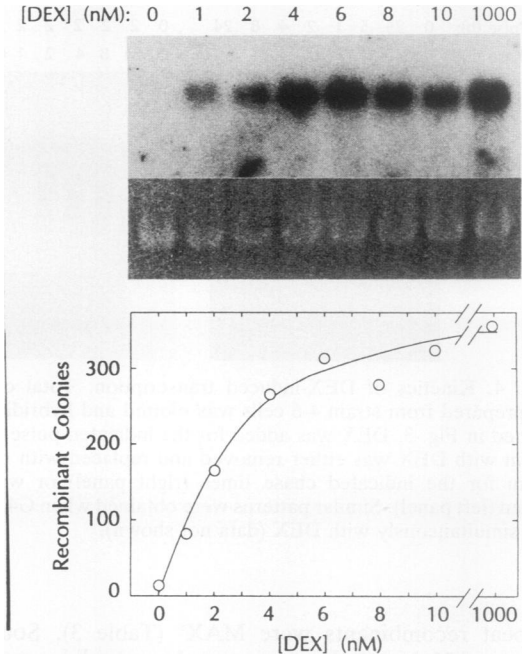

FIG. 7. Modulation of recombination levels and transcript levels with various concentrations of DEX. (Top) Strain 4-6 was incubated in the presence of increasing concentrations of DEX, and total RNA was analyzed as described in the legend to Fig. 3. (Bottom) The total numbers of G418^r recombinants in three dishes are plotted for various concentrations of DEX.

similar to that described here demonstrated that transcription stimulates crossovers but not gene conversions (26, 27). These disparate results suggest that recombination mechanisms may be influenced by additional factors such as the structure and location of recombination substrates. In CHO cells, physical mapping of recombinant products of direct repeats clearly showed that transcription stimulates homologous recombination (Fig. 5). Transcription also stimulated homologous recombination between inverted repeats, forming MMTV *neo*$^+$ genes, although additional nonhomologous recombination events may have produced other complex rearrangements with inverted repeats (Fig. 6). These results suggest that inappropriate high-level transcription of repeated elements might cause deleterious genetic rearrangements (see below).

Inactivation of inverted SV*gpt* genes: an antisense switch? About 15% of inverted-repeat recombinants unexpectedly inactivated the SV*gpt* gene, and physical analyses suggested that these products may result from crossovers or unequal sister chromatid exchanges. One explanation for this result is that rearranged SV40 promoters may be inactivated by promoter occlusion (7, 8, 12). Alternatively, the absence of transcription termination and polyadenylation signals in MMTV *neo*$^+$ genes produced by crossovers (or unequal exchanges) might yield antisense *gpt* mRNA that blocks *gpt* translation (Fig. 8). (In stable transfection assays, transcription termination and polyadenylation signals were not essential for functional expression of G418 resistance [unpublished results].) Thus, this system might be acting as an antisense switch. An antisense switch might prove valuable if tissue-specific recombination signals (such as those in

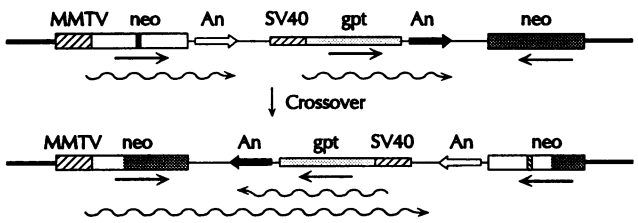

FIG. 8. An antisense switch. *neo* repeats in parent cells are drawn as open and shaded boxes (above) to allow differentiation in the crossover product (below). The MMTV *neo* mutation (black bar) may or may not be present in the recombinant depending on whether gene conversion accompanies the crossover (shown as hatched bar). Transcription termination-polyadenylation signals (An) are shown for MMTV *neo* (white arrow) and SV*gpt* (black arrow), and predicted mRNAs are shown by wavy lines for the parent and crossover product. Antisense mRNA extends through *gpt* in the crossover product.

immunoglobulin genes) were used, permitting tissue-specific regulation of antisense expression.

Possible mechanisms of transcription-enhanced recombination. The earliest model to explain transcription-enhanced recombination was proposed by Ikeda and Matsumoto (10) to account for results with phage λ. This model suggested that RNA polymerase-mediated strand-separation promoted pairing of homologous regions. Alternatively, transcription may increase the accessibility of a region to nuclease attack, as suggested for HO nuclease cleavage of the yeast mating type locus (15), and nuclease cleavage prior to V(D)J joining (1, 2). However, some data indicate that transcription may inhibit HO nuclease cleavage at non-*MAT* loci (20). Although it is reasonable to suppose that increased accessibility of transcribed regions to specific nucleases might facilitate nuclease cleavage, the role of double-strand breaks in general transcription-enhanced recombination remains unclear.

An alternative set of models draws on the evidence that transcription promotes supercoiling (32). These models suggest that transcription-mediated alterations in DNA conformation may stimulate recombination and are consistent with evidence suggesting that topoisomerases suppress recombination (for a review, see reference 33). For example, yeast *top1/top2* double mutants frequently recombine highly transcribed rDNA repeats, yielding large numbers of extrachromosomal rings. Reactivating topoisomerases in these mutants causes rings to reinsert into their original positions (4, 14). Furthermore, *top3* mutants are hyperrecombinogenic for repeated TY elements (31). These findings suggest that recombination and topoisomerase activity represent alternative mechanisms for relieving torsional stress created by transcription-induced supercoiling. Because supercoiling increases DNA density, transcription-induced supercoiling may stimulate recombination by bringing repeated regions closer together, facilitating strand exchange. Topoisomerases recruited to relax transcription-induced supercoils may mediate recombination directly through strand cleavage and rejoining activities, but this possibility is inconsistent with the *top1/top2* results described above.

Genetic implications for transcription-enhanced intrachromosomal recombination. The demonstration that transcription stimulates intrachromosomal recombination in mammalian cells has several important genetic implications. First, transcription may influence specific gene rearrangements, such as those seen with yeast mating type genes and mammalian antibody genes. Second, as suggested by Keil and Roeder (13), intrachromosomal gene conversion between repeated elements may help to maintain homogeneity between members of multigene families. Finally, since recombination can cause potentially mutagenic rearrangements or deletions, it is possible that transcription-enhanced recombination might underlie genome instability associated with tumorigenesis. Many oncogenes encode either transcription factors (6) or products that regulate transcription through signal transduction pathways (3), raising the possibility that oncoprotein-mediated increases in transcription could increase genome-wide recombination and destabilize the genome. Genome instability, in turn, might produce the additional mutations required for growth-deregulated cells to progress to a tumorigenic state.

ACKNOWLEDGMENTS

The expert technical assistance provided by Douglas Sweetser and Win Ping Deng and helpful comments from Howard Liber, Karl Kelsy, John Little, F. Andrew Ray, and Richard Reynolds are greatly appreciated.

This research was supported by grant CA 54079 from the National Institutes of Health.

REFERENCES

1. **Alt, F. W., T. K. Blackwell, R. A. Depinho, M. G. Reth, and G. D. Yancopoulos.** 1986. Regulation of genome rearrangement events during lymphocyte differentiation. Immunol. Rev. **89**:5–30.
2. **Blackwell, T. K., M. W. Moore, G. D. Yancopoulos, H. Suh, S. Lutzker, E. Selsing, and F. W. Alt.** 1986. Recombination between immunoglobulin variable region gene segments is enhanced by transcription. Nature (London) **324**:585–589.
3. **Bourne, H. R., and A. L. DeFranco.** 1989. Signal transduction and intracellular messengers, p. 97–124. *In* R. A. Weinberg (ed.), Oncogenes and the molecular origins of cancer. Cold Spring Harbor Laboratory Press, Cold Spring Harbor, N.Y.
4. **Christman, M. F., F. S. Dietrich, and G. R. Fink.** 1988. Mitotic recombination in the rDNA of *S. cerevisiae* is suppressed by the combined action of topoisomerases I and II. Cell **55**:413–425.
5. **Deng, W. P., and J. A. Nickoloff.** 1992. Site-directed mutagenesis of virtually any plasmid by eliminating a unique site. Anal. Biochem. **200**:81–88.

5a. **Deng, W. P., and J. A. Nickoloff.** Unpublished data.

6. **Eisenman, R. N.** 1989. Nuclear oncogenes, p. 175–221. *In* R. A. Weinberg (ed.), Oncogenes and the molecular origins of cancer. Cold Spring Harbor Laboratory Press, Cold Spring Harbor, N.Y.
7. **Emmerman, M., and H. M. Temin.** 1984. Genes with promoters in retrovirus vectors can be independently suppressed by an epigenetic mechanism. Cell **39**:459–467.
8. **Emmerman, M., and H. M. Temin.** 1986. Quantitative analysis of gene suppression in integrated retrovirus vectors. Mol. Cell. Biol. **6**:792–800.
9. **Grimm, C., P. Schaer, P. Munz, and J. Kohli.** 1991. The strong ADH1 promoter stimulates mitotic and meiotic recombination at the ADE6 gene of *Schizosaccharomyces pombe*. Mol. Cell. Biol. **11**:289–298.
10. **Ikeda, H., and T. Matsumoto.** 1979. Transcription promotes recA-independent recombination mediated by DNA-dependent RNA polymerase in Escherichia coli. Proc. Natl. Acad. Sci. USA **76**:4571–4575.
11. **Johnson, R. S., M. Sheng, M. E. Greenberg, R. D. Kolodner, V. E. Papaioannou, and B. M. Spiegelman.** 1989. Targeting of nonexpressed genes in embryonic stem cells via homologous recombination. Science **245**:1234–1236.
12. **Kadesch, T., and P. Berg.** 1986. Effects of the position of the simian virus 40 enhancer on expression of multiple transcription units in a single plasmid. Mol. Cell. Biol. **6**:2593–2601.
13. **Keil, R. L., and G. S. Roeder.** 1984. *cis*-acting, recombination-stimulating activity in fragment of the ribosomal DNA of *S. cerevisiae*. Cell **39**:377–386.
14. **Kim, R. A., and J. C. Wang.** 1989. A subthreshold level of DNA topoisomerases leads to the excision of yeast rDNA as extrachromosomal rings. Cell **57**:975–985.
15. **Klar, A. J. S., J. N. Strathern, and J. B. Hicks.** 1981. A position-effect control for gene transposition: state of the expression of yeast mating-type genes affects their ability to switch. Cell **25**:517–524.
16. **Lin, F.-L., K. Sperle, and N. Sternberg.** 1984. Model for homologous recombination during transfer of DNA into mouse L cells: role for DNA ends in the recombination process. Mol. Cell. Biol. **4**:1020–1034.
17. **Lin, Y. H., and R. L. Keil.** 1991. Mutations affecting RNA polymerase I-stimulated exchange and rDNA recombination in yeast. Genetics **127**:31–38.
18. **Mansour, S. L., K. R. Thomas, and M. R. Capecchi.** 1988. Disruption of the proto-oncogene *int-2* in mouse embryo-derived stem cells: a general strategy for targeting mutations to non-selectable genes. Nature (London) **336**:348–352.
19. **Nickoloff, J. A., and R. J. Reynolds.** 1990. Transcription stimulates homologous recombination in mammalian cells. Mol. Cell.

Biol. **10**:4837–4845.
20. **Nickoloff, J. A., J. D. Singer, M. F. Hoekstra, and F. Heffron.** 1989. Double-strand breaks stimulate alternative mechanisms of recombination repair. J. Mol. Biol. **207**:527–541.
21. **Ringold, G. M., K. R. Yamamoto, J. M. Bishop, and H. E. Varmus.** 1977. Glucocorticoid-stimulated accumulation of mouse mammary tumor virus RNA: increased rate of synthesis of viral RNA. Proc. Natl. Acad. Sci. USA **74**:2879–2883.
22. **Sambrook, J., E. F. Fritsch, and T. Maniatis.** 1989. Molecular cloning: a laboratory manual, 2nd ed. Cold Spring Harbor Laboratory Press, Cold Spring Harbor, N.Y.
23. **Shenkar, R., M. H. Shen, and N. Arnheim.** 1991. DNase I-hypersensitive sites and transcription factor-binding motifs within the mouse Eβ meiotic recombination hot spot. Mol. Cell. Biol. **11**:1813–1819.
24. **Southern, P. J., and P. Berg.** 1982. Transformation of mammalian cells to antibiotic resistance with a bacterial gene under control of the SV40 early region promoter. J. Mol. Appl. Genet. **1**:327–341.
25. **Stewart, S. E., and G. S. Roeder.** 1989. Transcription by RNA polymerase I stimulates mitotic recombination in *Saccharomyces cerevisiae*. Mol. Cell. Biol. **9**:3464–3472.
26. **Thomas, B. J., and R. Rothstein.** 1989. Elevated recombination rates in transcriptionally active DNA. Cell **56**:619–630.
27. **Thomas, B. J., and R. Rothstein.** 1989. The genetic control of direct-repeat recombination in *Saccharomyces*: the effect of *rad52* and *rad1* on mitotic recombination at *GAL10*, a transcriptionally regulated gene. Genetics **123**:725–738.
28. **Voelkel-Meiman, K., R. L. Keil, and G. S. Roeder.** 1987. Recombination-stimulating sequences in yeast ribosomal DNA correspond to sequences regulating transcription by RNA polymerase I. Cell **48**:1071–1079.
29. **Voelkel-Meiman, K., and G. S. Roeder.** 1990. A chromosome containing HOT1 preferentially receives information during mitotic interchromosomal gene conversion. Genetics **124**:561–572.
30. **Voelkel-Meiman, K., and G. S. Roeder.** 1990. Gene conversion tracts stimulated by HOT1-promoted transcription are long and continuous. Genetics **126**:851–867.
31. **Wallis, J. W., G. Chrebet, G. Brodsky, M. Rolfe, and R. Rothstein.** 1989. A hyper-recombination mutation in S. cerevisiae identifies a novel eukaryotic topoisomerase. Cell **58**:409–419.
32. **Wang, J. C.** 1985. DNA topoisomerases. Annu. Rev. Biochem. **54**:665–697.
33. **Wang, J. C., P. R. Caron, and R. A. Kim.** 1990. The role of DNA topoisomerases in recombination and genome stability: a double-edged sword? Cell **62**:403–406.
34. **Young, H. A., T. Y. Shih, E. M. Scolnick, and W. P. Parks.** 1977. Steroid induction of mouse mammary tumor virus: effect upon synthesis and degradation of viral RNA. J. Virol. **21**:139–146.